Surface electronic structures of lithium nickel oxide solid solutions: selective methane oxidation

T. Miyazaki, R. Sumii, H. Tanaka, K. Amemiya & S. Hino

Research on Chemical Intermediates

ISSN 0922-6168

Res Chem Intermed
DOI 10.1007/s11164-014-1820-5

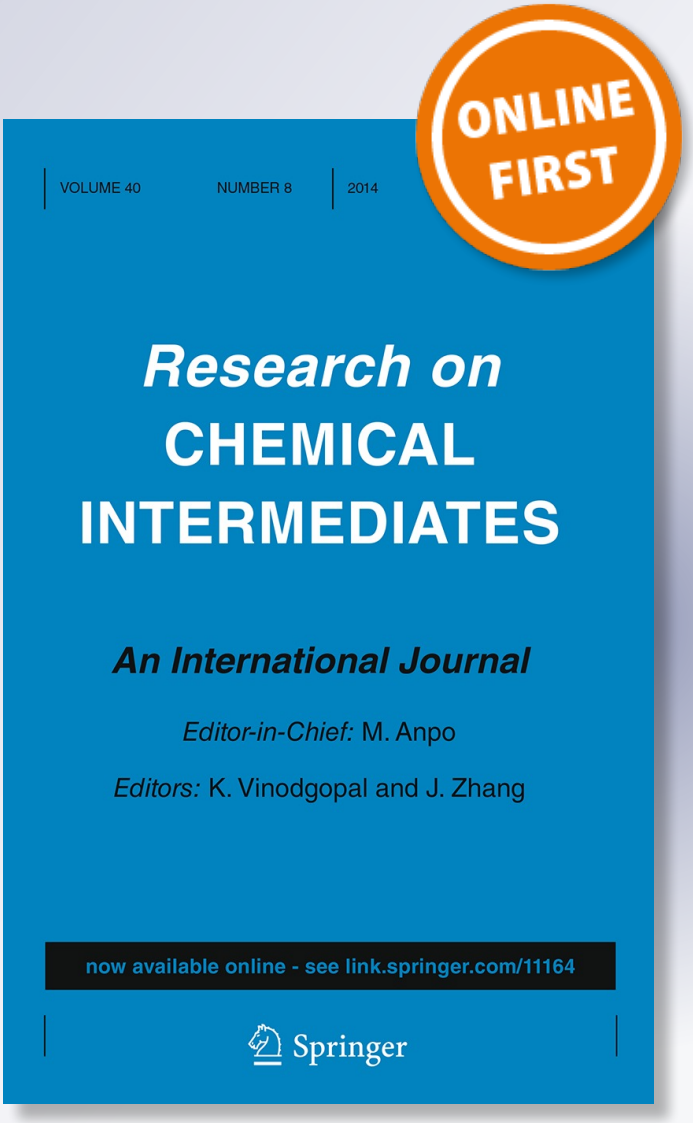

Res Chem Intermed
DOI 10.1007/s11164-014-1820-5

Surface electronic structures of lithium nickel oxide solid solutions: selective methane oxidation

T. Miyazaki · R. Sumii · H. Tanaka · K. Amemiya · S. Hino

Received: 23 June 2014 / Accepted: 20 September 2014

Abstract Ultraviolet photoelectron spectra (UPS) of lithium nickel oxide ($Li_xNi_{2-x}O_2$, $0 < x \leq 1.0$) solid solution were measured using a synchrotron radiation light source. The upper valence UPS are confirmed to consist of five structures for $E_b < 15$ eV. The electronic density of two O2p states changed as the compositional ratio of Li and Ni. After a contact reaction of $LiNiO_2$ and methane gas, the peak intensity of one of two O2p states decreased remarkably. It was found that the surface oxygen at the lower binding energy was selectively contributed to dissociate σ-bond between carbon and hydrogen of methane.

Keywords Lithium nickel oxides · Ultraviolet photoemission spectroscopy · Valence band structure · Oxidative coupling of methane · Selective oxidation

Introduction

An oxidative coupling of methane (OCM) is directly to convert methane to ethane and ethylene, which are used as raw materials of chemicals. This reaction may prove to be a viable alternative process to obtain higher hydrocarbons (C_{2+}) from

T. Miyazaki (✉) · H. Tanaka · S. Hino
Graduate School of Science and Engineering,
Ehime University, Matsuyama, Ehime 790-8577, Japan
e-mail: miyazaki@eng.ehime-u.ac.jp

R. Sumii
Institute for Molecular Science, Ultraviolet Synchrotron Orbital Radiation Facility (UVSOR),
Okazaki, Aichi 444-8577, Japan

R. Sumii · K. Amemiya
Institute for Materials Structure Science, High Energy Accelerator Research Organization
(KEK-PF), Tsukuba, Ibaraki 305-0801, Japan

Published online: 17 October 2014

methane gas in the future. Up to now, a large number of spherical support catalysts such as Li/MO (M = Mg, Ca, Sr), CaO–MnO/CeO_2, and Na_2WO_4/Mn/SiO_2 [1–6] and rare earth metal oxide catalysts such as La_2O_3, Sm_2O_3, and $Bi_{1.5}Y_{0.3}Sm_{0.2}O_{3-\delta}$ [7, 8] have been reported for this reaction. It is very important to understand selective partial oxidation on the OCM catalysts. It has been thought that the OCM reaction consists of several processes: (i) a generation of radicals such as $*CH_3$ and $*CH_2$ by breakage of the C–H bond of CH_4, (ii) a release of radical species from the surface of the catalyst, and (iii) a coupling process from two $*CH_3$ to C_2H_6 or two $**CH_2$ to C_2H_4. On the active site for the OCM reaction, surface oxygen species such as O^-, O_2^-, and O_2^{2-} have been proposed to activate methane [5, 9]. However, since the activation of methane is very difficult due to its chemical stability, very high temperature conditions are necessary to dissociate the C–H bond of CH_4. Additionally, an elucidation of the origin of selective catalysis is very difficult to apply to several surface analysis techniques because of active sites hidden inside the interface and the high temperatures involved.

Lithium nickel oxide functions as a redox (reduction/oxidation) catalyst for the OCM. The catalytic activity of the $Li_xNi_{2-x}O_2$ ($0 \leq x \leq 1.0$) solid solution has been studied for this purpose [10]. $Li_xNi_{2-x}O_2$ ($0 \leq x < 0.6_5$) has a cubic structure and combusts methane to carbon dioxide. On the other hand, $Li_xNi_{2-x}O_2$ ($0.6_5 \leq x \leq 1.0$) has a hexagonal structure and selectively converts methane to ethane and ethylene. Thus, hexagonal lithium nickel oxide (H-$LiNiO_2$) can selectively convert methane to a C_{2+} hydrocarbon. We have investigated the valence band structure of H-$LiNiO_2$, considering it as a model compound for the OCM reaction. In these results, two kinds of selective oxidation sites can be anticipated on lithium nickel oxide: One is the OCM active site, which partially dissociates one or two hydrogen atoms from methane, and another is a deep oxidation site, which converts methane to carbon oxide.

Ultraviolet photoelectron spectroscopy (UPS) was applied to investigate selective methane oxidation sites in order to understand partial oxidation for the OCM reaction. In this paper, the semi-ambient valence UPS was presented in order to clarify the origin of selective catalysis of $Li_xNi_{2-x}O_2$ ($0 \leq x \leq 1.0$) solid solution.

Experimental

$Li_xNi_{2-x}O_2$ ($x = 0.1, 0.3, 0.5, 0.7, 0.8$, and 1.0) solid solution were synthesized by a solid-state reaction. Mixtures of corresponding amounts of $LiNO_3$ and $Ni(OH)_2$ were ground and pressed into pellets, and heated in air at 873 and 1,073 K in a tube furnace. The reduction process of NiO and $LiNiO_2$ in methane or hydrogen atmosphere was studied by using thermogravimetric analysis (TGA, Shimadzu TGA-51). Ultraviolet photoelectron spectra (UPS) were measured using photoelectron spectroscopy equipment at the beam line BL8B2 at the UVSOR facility of the Institute for Molecular Science. The sample pellets were fixed on a copper substrate for good electrical contact. The Fermi energy (E_F) of the UPS system was determined by using the Fermi edge of gold. The total resolution was found to be 150 meV in the photon energy region of $20 \leq h\upsilon \leq 60$ eV. Surface treatment and

purification of the sample were carried out by argon ion sputtering and/or heating at 823 K, respectively. On the other hand, semi-ambient UPS were measured using photoelectron spectroscopy equipment at the beam line BL-7A at the Photon Factory in the High Energy Acceleration Organization (KEK-PF). The base pressure of the UPS measurement chamber was 5×10^{-7} Pa. The sample pellets were fixed on a Ta substrate that was also utilized as a resistant heater. The surface temperature of these samples was measured using a radiation thermometer. The temperature error was estimated to be ±5° or less. The semi-ambient valence band UPS of H-$LiNiO_2$ were measured under methane gas (99.9 % purity) at 5×10^{-3} Pa and 1,023 K.

Results and discussion

Powder X-ray diffraction patterns of $Li_xNi_{2-x}O_2$ ($x = 0.1$, 0.3, 0.5, 0.7, 0.8, and 1.0) were measured and no extra reflections of any impurities were detected. The diffraction patterns of the $Li_xNi_{2-x}O_2$ ($x \leq 0.6$) samples were assigned to a cubic structure, and those of the $Li_xNi_{2-x}O_2$ ($0.6 \leq x \leq 1.0$) samples were assigned to a hexagonal structure. In the case of $Li_xNi_{2-x}O_2$ ($x < 0.6$), Ni ions in (111) planes are partially substituted by Li ions that are randomly configured in these planes. On the other hand, the structure of $Li_xNi_{2-x}O_2$ ($0.6 < x < 1.0$) seems to be an incomplete hexagonal type. The incomplete hexagonal structure has alternately arranged Ni ion layers and a mixture of Li + Ni (Li $\gg$ Ni) layers. The crystal structure of $Li_xNi_{2-x}O_2$ solid solution and the high temperature dependence had been reported and the relationship between the structure, and the selectivity for the OCM reaction had been discussed in detail [10–12]. It has been confirmed that a hexagonal structure of $LiNiO_2$ was significantly held to 1,073 K, although the diffraction angle was shifted to a slightly lower angle at higher temperatures. TGA profiles of NiO and $LiNiO_2$ in methane or hydrogen atmosphere are shown in Fig. 1. In the case of NiO in methane gas, the weight begins to loss at 780 K for a dissociation of hydroxide. Then, the weight of NiO begins to increase at 875 K for carbon deposits on nickel metal, which is generated from NiO. In the case of $LiNiO_2$ in methane gas, the weight slightly increases at 750–1,040 K. The weight gain seems to be an absorption process of methane on $LiNiO_2$ surface. Then, the weight begin to loss at 1,040 K for a dissociation of hydroxide, which is generated from the absorbed methane. Also, it seems that $LiNiO_2$ is easy to be reduced by hydrogen since the weight of $LiNiO_2$ begins to loss at 700 K. These findings may indicate that the activation of methane seems to be more efficient on the surface of NiO than $LiNiO_2$. However, these functions that are advantageous to activation should become to completely oxidize methane to carbon oxide. We could not easily explain this only from these results. The reduction processes of $LiNiO_2$ by methane are significantly different from that of NiO. The origin of their differences could be clarified by understanding the valence electronic structure of $Li_xNi_{2-x}O_2$ solid solution in detail. The valence band structures were measured and were traced to change in methane atmosphere.

The upper valence UPS of $Li_{0.1}Ni_{1.9}O_2$, $Li_{0.3}Ni_{1.7}O_2$, $Li_{0.5}Ni_{1.5}O_2$, $Li_{0.6}Ni_{1.4}O_2$, $Li_{0.8}Ni_{1.2}O_2$, and $LiNiO_2$ obtained with $h\upsilon = 40$ eV incident photon energy are

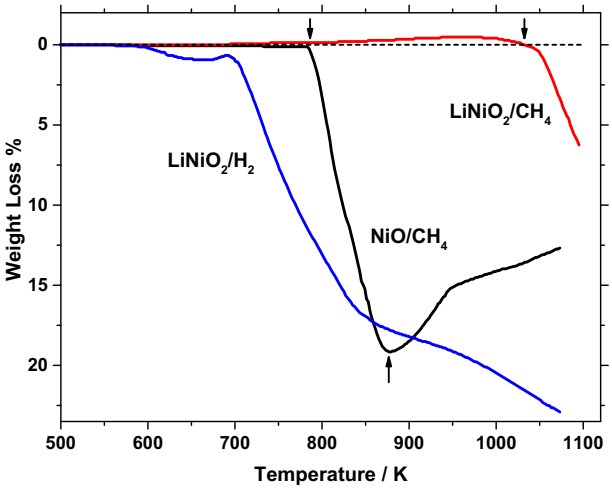

Fig. 1 TGA profiles of **a** $LiNiO_2$ under methane gas, **b** $LiNiO_2$ under hydrogen gas, and **c** NiO under methane gas

shown in Fig. 2. Five structures can be distinguished from the Fermi level to $E_b = 15$ eV, denoted by the characters α–ε. These appear to have distinct differences in the peak top position, interval, and intensity. The spectral onset energies of $Li_xNi_{2-x}O_2$ ($0 \leq x \leq 1.0$) changes at 0.2–1.1 eV. When their UPS are compared with each other in detail, the correspondence can be found in two groups: group A consisting of $Li_{0.1}Ni_{1.9}O_2$, $Li_{0.3}Ni_{1.7}O_2$, and $Li_{0.5}Ni_{1.5}O_2$ and group B consisting of $Li_{0.6}Ni_{1.4}O_2$, $Li_{0.8}Ni_{1.2}O_2$, and $LiNiO_2$. The UPS of the group A shifted toward the lower binding energy side as Li content increases. On the other hand, the UPS structures of group B shift to the higher energy side and correspond to changing electronic structure from a cubic structure to a hexagonal structure. The ionization potential of group B also becomes small as the lithium content increases. In addition, the intensity of peak α and β of $Li_{0.8}Ni_{1.2}O_2$ and $LiNiO_2$ in group B decreases as the Li content increases. Thus, there is considerable evidence to show a change in the electronic structure of $Li_xNi_{2-x}O_2$ ($0 < x \leq 1.0$) at around $x = 0.6$.

The upper valence bands of $Li_xNi_{2-x}O_2$ ($0 < x \leq 1.0$) are derived from the Ni3d and O2p states, and have no contribution of the Li1s at 54.7 eV. The UPS of $Li_xNi_{2-x}O_2$ ($x = 0.1$, 0.5, 0.8, and 1.0) with their Gaussian fitting curves are shown in Fig. 3. These spectra for $Li_{0.1}Ni_{1.9}O_2$, $Li_{0.5}Ni_{1.5}O_2$, $Li_{0.8}Ni_{1.2}O_2$, and $LiNiO_2$ consistently matched the Gaussian fitting curve after smooth background subtraction of secondary electrons from each spectrum. The calculated spectra made from five individual bands consistently matched the UPS of $Li_xNi_{2-x}O_2$. The full width at half maximum for each of the five peaks was within 1.5–2.5 eV as the results of Gaussian-free parameters. The peak top positions of $LiNiO_2$ were centered at $E_b = 1.8$, 3.0, 5.0, 7.0, and 10.2 eV and were comparable to those of $Li_{0.1}Ni_{1.9}O_2$, $Li_{0.5}Ni_{1.5}O_2$, and $Li_{0.8}Ni_{1.2}O_2$. When Ni^{2+} ions in NiO are replaced with Li^+ ions, the electronic density of the Ni3d (e_g) states should change as a result of electronic

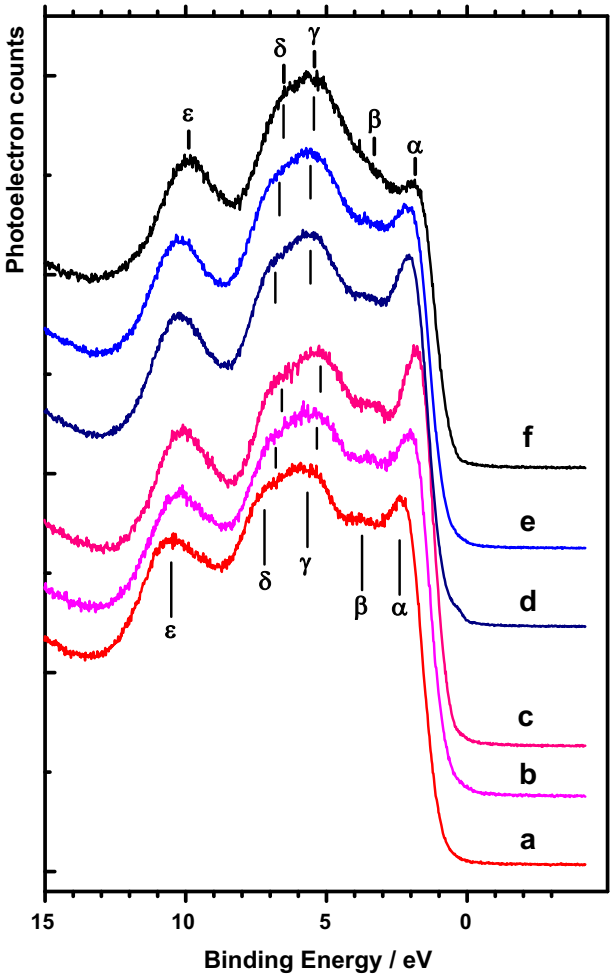

Fig. 2 Ultraviolet photoemission spectra of **a** $Li_{0.1}Ni_{1.9}O_2$, **b** $Li_{0.3}Ni_{1.5}O_2$, **c** $Li_{0.5}Ni_{1.5}O_2$, **d** $Li_{0.6}Ni_{1.4}O_2$, **e** $Li_{0.8}Ni_{1.2}O_2$, and **f** $LiNiO_2$ obtained with $h\upsilon = 40$ eV incident photon energy

charge compensation which would produce Ni^{3+} ($Ni3d^7$) in the solid. The substitution from Ni^{2+} to Li^+ resulted in the formation of Ni^{3+} and should be expected to influence the electronic structures of the O2p states. This indicates that the area intensity ratio of γ to δ was 2:1 for $Li_{0.1}Ni_{1.9}O_2$ (Fig. 3a), almost unity for $Li_{0.5}Ni_{1.5}O_2$ (Fig. 3c), 1:2 for $Li_{0.8}Ni_{1.2}O_2$ (Fig. 3e), and 1:5 for $LiNiO_2$ (Fig. 3f). Thus, the formation of Li^+ and Ni^{3+} ions and the change from a cubic to hexagonal structure would be reflected by the electronic structures of the $Li_xNi_{2-x}O_2$ solid solution.

The upper valence UPS of $LiNiO_2$ obtained with $h\upsilon = 30$ eV incident photon energy are shown in Fig. 4a. The upper valence UPS ($E_b \leq 15$ eV) consists of several structures, denoted by characters α'–ε'. These structures could be assigned

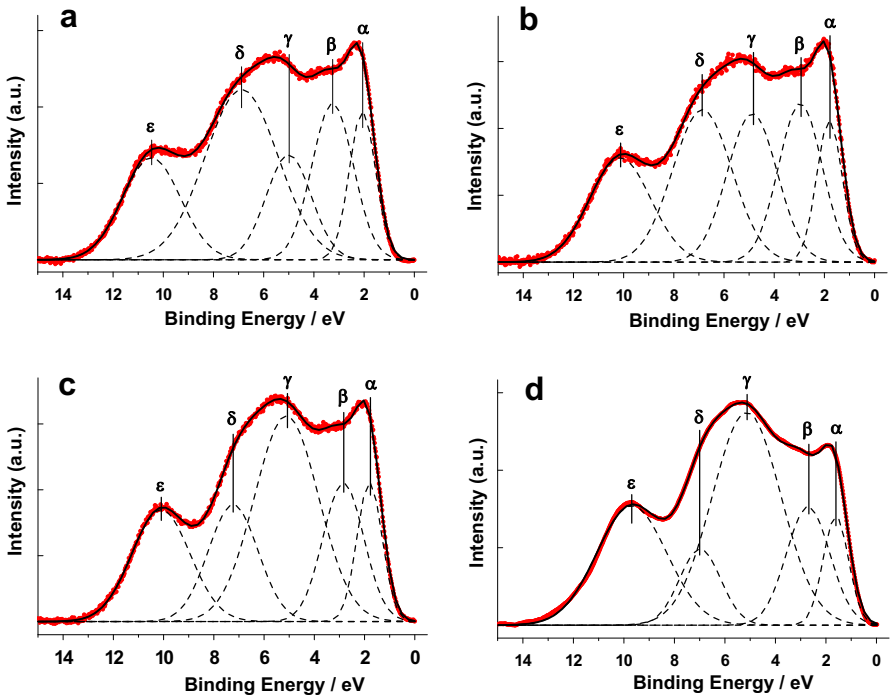

Fig. 3 Ultraviolet photoemission spectra and corresponding Gaussian-fitted curve for (**a**) $Li_{0.1}Ni_{1.9}O_2$, (**b**) $Li_{0.5}Ni_{.5}O_2$, (**c**) $Li_{0.8}Ni_{1.2}O_2$, and (**d**) $LiNiO_2$ obtained with $h\upsilon = 40$ eV incident photon energy

to two Ni3d (α' and β') states, two O2p (γ' and δ') states, and the Ni3d satellite (ε') [11]. When the sample pellet of $LiNiO_2$ was heated to 1,023 K (Fig. 4b), the intensity of the two Ni3d states decreased in comparison with other peaks. The intensity of the two O2p states (γ' and δ') became clearly distinguishable by the heat treatment. The peak intensity ratio of γ' and δ' was almost unity, as seen in Fig. 4b. When the $LiNiO_2$ sample contacted with methane gas, the peak intensity of one of two O2p states discriminately decreased compared to the other peak (Fig. 4c). This suggested that the O2p (γ') state of $LiNiO_2$ might play a role in the dehydrogenation of methane in the first step of the OCM reaction. Significantly, two O2p states with the different binding energy was confirmed and coexisted on $LiNiO_2$. These findings indicate that one of these states could activate methane for the OCM reaction, and another site might function as absorbing transient intermediates such as methyl radicals since the weight gain of $LiNiO_2$ could be observed in TGA profile. The role of the surface lattice oxygen for selective oxidation of methane might be found out in the valence band structure for the first time. Furthermore, we need to study the top valence band structure in detail in order to clarify the origin of selective catalysis and to establish advanced reaction control technology.

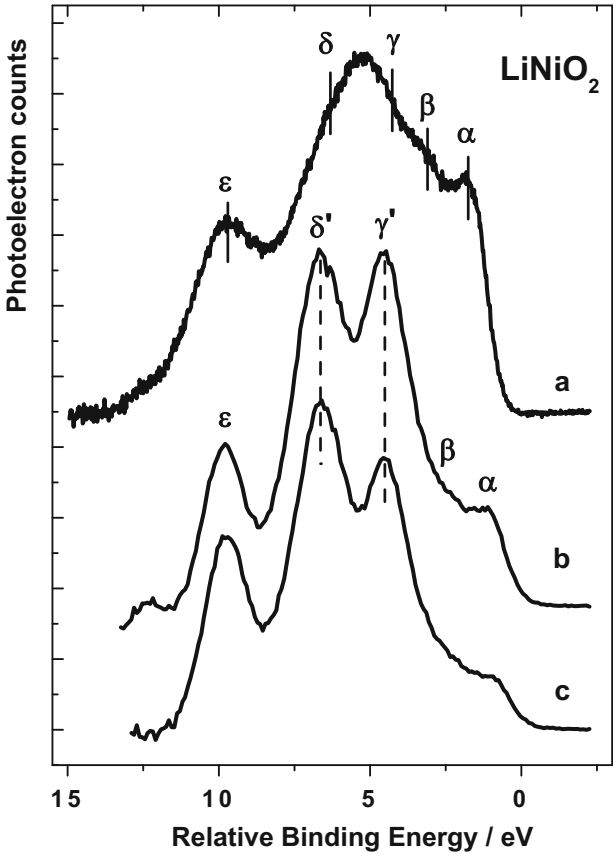

Fig. 4 Valence band UPS of $LiNiO_2$ at (*a*) room temperature after argon ion sputtering, (*b*) 1,023 K, and (*c*) 1,023 K in methane gas of 5×10^{-3} Pa. These spectra were obtained with $h\upsilon = 30$ eV incident photon energy

In this work, we present the upper valence UPS of the $Li_xNi_{2-x}O_2$ ($0 < x \leq 1$) solid solution and their Gaussian-fitting curves. The electronic structure of $Li_xNi_{2-x}O_2$ ($x < 0.6$) with a cubic structure is different from that of $Li_xNi_{2-x}O_2$ ($x > 0.6$) with a hexagonal structure. Also, it could be shown in the semi-ambient valence UPS that the O2p states at the low binding energy activated methane in the contact reaction. These results indicate that the $Li_xNi_{2-x}O_2$ catalyst should depend on the valence band structure and selective catalysis for the OCM reaction.

Acknowledgments The authors acknowledge the staff of the UVSOR Facility of the Institute for Molecular Science and the Photon Factory for their helpful advice and technical support. The present study has been performed under the approval of the Photon Factory Advisory Committee (PF PAC No. 2009G615).

References

1. G.E. Keller, M.M. Bhasin, J. Catal. **73**, 9–19 (1982)
2. M. Hatano, K. Otsuka, Inorg. Chim. Acta **146**, 243–247 (1988)
3. M. Gaffney, C.A. Jones, J.J. Leonard, J.A. Sofranko, J. Catal. **114**, 422–432 (1988)
4. L. Mleczko, M. Baerns, Fuel Process. Technol. **42**, 217–248 (1995)
5. J.H. Lunsford, Angew. Chem. **34**, 970–980 (1995)
6. N.G. Maksimov, G.E. Selyutin, A.G. Anshits, E.V. Kondratenko, V.G. Roguleva, Catal. Today **42**, 279–281 (1998)
7. A.G. Dedov, A.S. Loktev, I.I. Moiseev, A. Aboukais, J.F. Lamonier, I.N. Filimonov, Appl. Catal. A **245**, 209–220 (2003)
8. Y. Zeng, F.T. Akin, Y.S. Lin, Appl. Catal. A **213**, 33–45 (2001)
9. T. Ito, J.-X. Wang, C.-H. Lin, J.H. Lunsford, J. Am. Chem. Soc. **107**, 5062–5068 (1985)
10. T. Miyazaki, T. Doi, M. Kato, T. Miyake, I. Matsuura, Appl. Surf. Sci. **121**(122), 492 (1997)
11. T. Miyazaki, D. Yoshimura, K. Okudaira, Appl. Catal. A **38**, 79–82 (2008)
12. T. Miyazaki, T. Doi, T. Miyamae, I. Matsuura, Stud. Surf. Sci. Catal. **110**, 245–254 (1997)